EPJ Web of Conferences **321**, 01009 (2025) https://doi.org/10.1051/epjconf/202532101009
APITECH-VII-2025

Mathematical model for studying frequency response of a buck-boost DC/DC converter

Alexey Andriyanov*

Bryansk State Technical University, Bulvar 50-let Oktyabrya, Bryansk, 241035, Russia

Abstract. The paper is devoted to the development of a high-speed nonlinear dynamic mathematical model of a direct inverting voltage converter designed to remove its low-signal frequency response, namely: open loop transmission coefficient, input conductivity, output resistance of the converter. The study focus is a direct inverting voltage converter with output voltage feedback having a proportional regulator in the loop stabilization circuit and generators of sinusoidal measuring effects as part of the circuit. The paper gives a mathematical model of the converter which is a system of differential and nonlinear transcendental equations. The proposed model belongs to numerical and analytical ones, where at certain time intervals processes are described by a system of linear differential equations. This approach allows to significantly speed up the calculation of frequency response of the converter in comparison with standard software using numerical integration methods. The paper gives the results of calculating the frequency response and compares with the results obtained using verified software. The analysis shows the correctness of the developed mathematical model. The proposed approach has not been considered before, and the use of a nonlinear mathematical model allows to take into account the nonlinearity of the object under study.

1 Introduction

Secondary supply sources (SSS) with constant output voltage are widely used in many fields of activity to ensure the operation of various electronic devices. SSSs are developed on the basis of pulsed methods of power conversion, which fully satisfy the concept of miniaturization of such devices. Modern SSSs ensure the stability of output voltage under conditions of changes in the input voltage and load resistance due to the feedback on the output voltage [1-4]. When designing such systems, a comprehensive analysis of their frequency response is required [3].

One of the most important tasks at the development stage is the task of ensuring SSS stability by selecting regulator parameters, which is done using frequency analysis of a low-signal, linearized open loop model of the system. The main criterion of stability in this case is the Nyquist stability criterion, which involves the analysis of the bode plot (BAP) of an open loop. According to this criterion, the system is stable if BAP of the open loop on the complex plane does not bend around the following point (-1, 0) [5].

* Corresponding author: mail@ahaos.ru

It is also worth noting that power supply systems can be aggregated and include several power supply devices (PSD) connected differently. At the same time, each PSD as part of an aggregated power supply system (APSS) is a full-fledged device capable of solving its tasks outside APSS. The construction of such systems also faces the problem of stability, namely, structural stability, when some links of such a system are stable, but the system as a whole is not stable at all. For example, when two DC voltage sources are cascaded on, the structural stability of this system is analyzed based on bode plot analysis of the ratio $Z_{out1}(s)/Z_{in2}(s)$, where $Z_{out1}(s)$ is the output operating resistance of the first cascade, $Z_{in2}(s)$ is the input operating resistance of the second cascade.

Thus, when designing a DC secondary supply source, it is necessary to study the following frequency characteristics.

1. Frequency dependences of the module and phase of the open loop transmission coefficient of the system.
2. Frequency dependences of the module and phase of the input resistance (or conductivity) of the converter.
3. Frequency dependences of the module and phase of the output resistance of the converter.
4. Frequency dependences of the module and phase of the transmission coefficient of the converter.

As mentioned above, frequency dependencies (item 1) are used to select the parameters of the system controller. Frequency dependencies (items 2, 3) are used to analyze the structural stability of aggregated power supply systems. Frequency dependencies (item 4) are applied to analyze the transmission of interferences from SSS input to its output (this will not be considered in this paper).

Currently, analytical expressions have been obtained describing the frequency characteristics listed above [4, 6], which allow to evaluate the properties of the system in a small neighborhood of the operating point, that is typical for low-signal analysis. This analysis assumes the linearization of the system near the operating point, which leads to some loss of information about its properties.

In reality, pulse-width DC/DC voltage conversion systems are nonlinear dynamic systems which can have nonlinear oscillations with a frequency other than the conversion frequency, and the static control can also be significantly nonlinear [6-9]. As shown in [4], more accurate results are obtained by frequency characteristics taken on a nonlinear dynamic model of the system by applying a low-signal measuring effect with a given frequency and amplitude to a certain input of the circuit, followed by an assessment of the system's response at a given output of the circuit and calculating the ratio of the amplitude of the output signal to the amplitude of the disturbance signal. It is noted in [4] that the frequency characteristics obtained in this way may differ from the frequency characteristics obtained using analytical expressions. At the same time, the differences found [4] allow to consider the inaccuracy of the analytical approach to the analysis of these systems. In [4], the frequency characteristics were calculated using FastMean program, which uses numerical methods to calculate time dependencies. LTspice and MatLab Simulink programs can also be used for this task. Earlier, the author of this paper developed a specialized module for Simulink, which allows solving the task for converter models built in Simulink environment. However, it should be noted that using numerical methods to solve such problems (which is implemented in Simulink) significantly increases the calculation time, since in order to achieve the required accuracy it is necessary to reduce the integration step.

In this paper, to calculate the frequency response of pulse voltage converters, it is proposed to use the so-called piecewise-linear numerical and analytical model, which involves the use of a linear system of differential equations to describe electromagnetic processes at certain time intervals, each of which is associated with a certain set of on and

off circuit valves. In this case, the moment of transition from one interval to another is calculated using numerical methods for solving nonlinear equations. This will significantly increase the speed of calculating time dependencies. The mathematical model itself generally belongs to the class of nonlinear dynamic models.

As an object of research, the paper considers an SSS based on a direct inverting converter with pulse width modulation (PWM) [1].

2 Description of a loop automatic control system based on an inverting voltage converter with measuring actions generators

This section describes an automatic control system based on an inverting voltage converter, with measuring actions sources included in the circuit to calculate SSS frequency response. The system in Figure 1 is a classic SSS with output voltage feedback. The power section consists of *VT* – transistor with R_{vt} resistance, *VD* – power diode with R_{vd} resistance, *Ind* – inductor with L inductance and R_L resistance, *Cap* – capacitor with C capacity and R_c resistance. Also the diagram shows R_{LD} load resistance and U_{in} constant input voltage. SSS control system consists of FBSA – feedback signal amplifier with gain factor β, subtractor SB, proportional regulator R with α coefficient, clock generator MC, scanning voltage generator RG, comparator "==", trigger T, and DRV – driver. Figure 1 has the following signal designations: u_{ref} is master control, u_{err} is error signal, u_r is regulator output signal, u_{con} is control signal, u_{cmp} is output signal after PWM comparator, up is power transistor control signal, i_L is inductor current, u_c is capacitor voltage.

In Figure 1 (a) measuring actions sources used to calculate the required frequency characteristics are marked in red. To change a specific frequency response, one of the three inputs of the circuit is used, to which a measuring action is applied and one of the three outputs, from which the response of the system as an electrical signal is monitored. The input of the circuit to which the measuring action is applied, and the output from which the signal is taken to analyze the system response depends on the type of frequency response being calculated.

When calculating the coefficient of the gain open loop $K_{pg}(s)$, u_{prb} measuring action is introduced into the closed loop using AD adder. In this case, u_{con} disturbance signal will serve as an input signal of the open loop circuit, and u_r disturbance signal will be the output signal. Then the coefficient of the open loop in the operator form will be the following

$$K_{pg}(s) = \frac{u_r(s)}{u_{con}(s)}.$$

When calculating Yin input conductivity, $u_{inv}(t)$ measuring action (input signal) is added to the input DC voltage and the input current of the converter i_{in} (output signal) is analyzed. In this case, the input conductivity in the operator form looks like

$$Y_{in}(s) = \frac{i_{in}(s)}{u_{inv}(s)}.$$

Obviously, the input resistance is calculated as

$$Z_{in}(s) = \frac{1}{Y_{in}(s)}.$$

When calculating Z_{out} output resistance, $j_{outv}(t)$ alternating current source (input signal) is connected in parallel to the load and u_{out} output voltage of the converter (output signal) is analyzed as follows

$$Z_{out}(s) = \frac{u_{out}(s)}{j_{outv}(s)}.$$

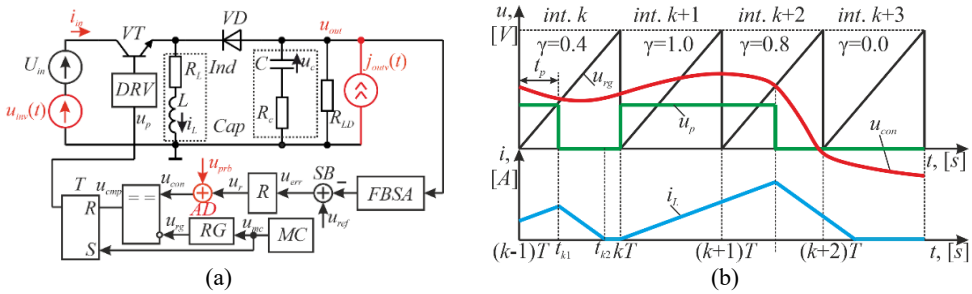

Fig. 1. Explanation of the equivalent circuit: (a) – equivalent circuit structure, (b) – time diagrams of the system signals.

The converter operation is widely described in the literature [1], so here we will give only a brief description in order to understand the principle of constructing a mathematical model.

Figure 1 (b) presents time diagrams characterizing the operating modes of the converter power section and the pulse width modulator of the control system. When the pulse voltage converter is in operation, the power switch is periodically switched with T period. The duration of the open state interval of the power switch determines the output voltage of the converter, which is characterized by PWM duty factor $\gamma=t_p/T$, the duration of the open state of the power switch within the clock interval (Figure 1, b).

The feature of the power section of pulse voltage converters is the immutability of its structure at a certain time interval of PWM clock interval. Moreover, each such subinterval is characterized by a certain state of *VT* transistor and *VD* diode. The inverting converter has generally three such subintervals within PWM clock interval.

Each PWM clock interval is characterized by k number. So, k-clock interval is located on the time interval from $(k–1)T$ to kT. Accordingly, k+1–clock interval will be located in the time interval from kT to $(k+1)T$ (clock interval numbers are signed on top of Figure 1, b).

Let us consider k clock interval (Figure 1, b). It is the most significant in this case. Firstly, at this clock interval, the duty factor $\gamma=0.4$, and, secondly, there is intermittent inductor current mode here, when it manages to drop to zero before the start of the next clock interval.

PWM clock interval in this case is divided into three subintervals. In this case, at the first subinterval from $(k–1)T$ to t_{k1}, *VT* transistor is open, *VD* diode is closed ($R_{vt}=R_{vton}$ и $R_{vd}=R_{vdoff}$) and i_L inductor current increases linearly. On the second subinterval from t_{k1} to t_{k2}, *VT* transistor is closed, *VD* diode is open ($R_{vt}=R_{vtoff}$ и $R_{vd}=R_{vdon}$), the inductor current decreases linearly. At t_{k2} moment, the third subinterval begins when the inductor current drops to zero. At t_{k2} moment, *VD* diode closes and until kT moment they both remain closed ($R_{vt}=R_{vtoff}$ и $R_{vd}=R_{vdoff}$). At k-clock interval, all possible switching in the circuit is implemented. R_{vton} and R_{vdon} here are resistances of the transistor and diode in the open state, R_{vtoff} and R_{vdoff} are resistances of the transistor and diode in the closed state.

At $(k+1)$-clock interval (Figure 1, b), the duty factor $\gamma=1.0$ and the inductor current increases over the entire clock interval, since *VT* power transistor is open all the time.

At $(k+2)$-clock interval (Figure 1, b), the inductor current does not have time to drop to zero (there is no t_{k2} moment), which refers to the continuous inductor current mode, i.e. in this case there is no interval where *VT* and *VD* are simultaneously closed.

At k+3- clock interval (Figure 1, b), the duty factor $\gamma=0$ and there is no inductor current rise interval.

3 Mathematical model of the system

When describing electromagnetic processes in the power section, we will use a power section equivalent circuit generalized for each subinterval of PWM clock interval, at which the structure of the power section is unchanged (Figure 2). Each *i*-subinterval of the immutability of the power section structure (*i*=1, 2, 3) is characterized by certain resistance values of the transistor and diode (R_{vti} and R_{vdi}, respectively), depending on the state of *VT* and *VD*, as mentioned above.

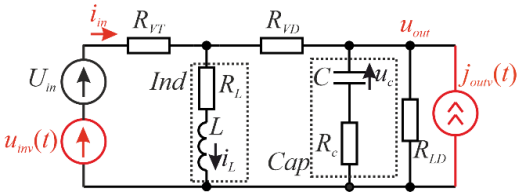

Fig. 2. Generalized equivalent circuit of the power section at i-subinterval of the immutability of the power section structure.

The equivalent circuit shown in Figure 2 can be described in the state space by a system of differential equations as follows

$$\begin{aligned}
&\frac{di_L}{dt} = -\frac{R_c\left[P + R_{LD}\left(R_{vt}(\mathbf{X},t) + R_L\right)\right] + R_{LD}P}{GL} i_L - \frac{R_{LD}R_{vt}(\mathbf{X},t)}{GL} u_c + \\
&+ \frac{R_cR_{LD} + R_{vd}(\mathbf{X},t)\left(R_c + R_{LD}\right)}{GL}\left(U_{in} + u_{inv}(t)\right) - \frac{R_cR_{LD}R_{vt}(\mathbf{X},t)}{GL} j_{outv}(t); \\
&\frac{du_c}{dt} = \frac{R_{LD}R_{vt}(\mathbf{X},t)}{GC} i_L - \frac{R_{LD} + R_{vd}(\mathbf{X},t) + R_{vt}(\mathbf{X},t)}{GL} u_c - \frac{R_{LD}}{GC}\left(U_{in} + u_{inv}(t)\right) + \\
&+ \frac{R_{LD}\left(R_{vt}(\mathbf{X},t) + R_{vd}(\mathbf{X},t)\right)}{GL} j_{outv}(t),
\end{aligned} \tag{1}$$

where measuring actions

$$u_{inv}(t) = u_{invm}\sin(\omega_{prb}t);$$
$$j_{outv}(t) = j_{outvm}\sin(\omega_{prb}t).$$

In this case, the output voltage is calculated using the following expression

$$u_{out} = \frac{R_{LD}R_c}{R_{LD} + R_c} i_L + \frac{R_{LD}}{R_{LD} + R_c} u_c. \tag{2}$$

Equations (1, 2) describing system processes can be expressed in vector-matrix way

$$\begin{aligned}
&\frac{d\mathbf{X}}{dt} = \mathbf{A}(\mathbf{X},t)\mathbf{X} + \mathbf{B}(\mathbf{X},t)\mathbf{u}(\mathbf{X},t); \\
&\mathbf{Y} = \mathbf{C}\mathbf{X},
\end{aligned} \tag{3}$$

where $\mathbf{X}=(i_L\ u_c)^T$ is a vector of state variables, $\mathbf{Y}=(u_{out}\ i_L)^T$ is an output vector, **A** is a system matrix, **B** is a control matrix, **C** is an output matrix, $\mathbf{u}(\mathbf{X},t)$ is a vector of control actions

As it can be seen from (3), **A** and **B** matrices depend not only on time, but also on the vector of state variables, which indicates the nonlinearity of the system under consideration.

The system of equations (3) for *i*-subinterval of the immutability of the power section structure (*i*=1, 2, 3) can be written in vectors and matrices

$$\begin{aligned}
&\frac{d\mathbf{X}}{dt} = \mathbf{A}_i\mathbf{X} + \mathbf{B}_i\mathbf{u}_i(t); \\
&\mathbf{Y} = \mathbf{C}\mathbf{X},
\end{aligned} \tag{4}$$

where $\mathbf{X}=(i_L, u_c)^T$ is a vector of state variables, $\mathbf{A}_i$ is a system matrix, $\mathbf{B}_i$ is a control matrix, $\mathbf{u}_i(t)$ is a vector of control actions, which in the smoothness region depends only on time.

Obviously, since the power section structure does not change at *i*-subinterval, $\mathbf{A}_i$ and $\mathbf{B}_i$ matrices do not change, i.e. the system (4) is linear. $\mathbf{A}_i$ and $\mathbf{B}_i$ matrices can be obtained from (1) by substituting R_{vt} and R_{vd} values characterizing *i*-subinterval and are not given in this paper due to some limitations.

The system (4) can be expressed as the following

$$\frac{d\mathbf{X}}{dt} = \mathbf{A}_i\mathbf{X} + \mathbf{B}_{consti}\mathbf{u}_{consti} + \mathbf{B}_{vari}\mathbf{u}_{vari}(t), \tag{5}$$

where $\mathbf{B}_{consti}$, $\mathbf{B}_{vari}$ are control matrices (not given in this paper due to some limitations), $\mathbf{u}_{consti}(\mathbf{X},t)$ is the vector of control actions, $\mathbf{u}_{vari}(\mathbf{X},t)$ is the vector of variable control actions.

Vectors of control actions in (5) are the following

$$u_{consti}(\mathbf{X},t) = \left[U_{in}\ \ 0\right]^T;$$

$$u_{vari}(\mathbf{X},t) = \left[u_{invm}\sin(\omega_{prb}t)\quad j_{outvm}\sin(\omega_{prb}t)\right]^T.$$

The solution (5) can be presented as vectors and matrices

$$\begin{aligned}\mathbf{X}(z) = {} & \mathrm{e}^{\mathbf{A}_i(z-z_{k(i-1)})a}\mathbf{X}_{ici} + \left(\mathrm{e}^{\mathbf{A}_i(z-z_{k(i-1)})a} - \mathbf{E}\right)\mathbf{A}_i^{-1}\mathbf{B}_{consti}\mathbf{u}_{consti}(\mathbf{X},z) - \\ & \left(\mathbf{E}\omega_{prb}{}^2 + \mathbf{A}_i^2\right)^{-1}\left[\left(\mathbf{B}_{vari}\mathbf{u}'_{vari}(z)\omega_{prb} + \mathbf{A}_i\mathbf{B}_{vari}\mathbf{u}_{vari}(z)\right) - \right. \\ & \left. -\mathrm{e}^{\mathbf{A}_i(z-z_{k(i-1)})a}\left(\mathbf{B}_{vari}\mathbf{u}'_{vari}(z_{k(i-1)})\omega_{prb} + \mathbf{A}_i\mathbf{B}_{vari}\mathbf{u}_{vari}(z_{k(i-1)})\right)\right].\end{aligned} \tag{6}$$

In (6), a transition is made to the relative time, which for k-clock interval can be defined as

$$z = \frac{t-(k-1)T}{T},$$

where t is the absolute time. Within the clock interval, z varies from 0 to 1. Also in (6) $z_{(k\text{-}1)i}$ is the beginning of *i*–subinterval of the immutability of the power section structure in relative time, $\mathbf{X}_{ici}$ is the vector of state variables at $z_{(k\text{-}1)i}$ moment, $\mathbf{E}$ is a 2x2 unit matrix.

Also, after the transition to relative time, control actions vectors for the k-clock interval are the following

$$u_{consti}(\mathbf{X},z) = \left[U_{in}\ \ 0\right]^T;$$

$$u_{vari}(\mathbf{X},z) = \left[u_{invm}\sin\left(\omega_{prb}\left((k-1)T+zT\right)\right)\quad j_{outvm}\sin\left(\omega_{prb}\left((k-1)T+zT\right)\right)\right]^T.$$

Also in (6)

$$u'_{vari}(\mathbf{X},z) = \left[u_{invm}\cos\left(\omega_{prb}\left((k-1)T+zT\right)\right)\quad j_{outvm}\cos\left(\omega_{prb}\left((k-1)T+zT\right)\right)\right]^T.$$

When calculating time dependencies, fitting method is used, when on *i*-subinterval the calculation is based on (6), and when switching to *i*+1-subinterval, the vector of state variables at the end of *i*-subinterval is the vector of initial conditions $\mathbf{X}_{ici+1}$ for *i*+1-subinterval.

To move to the next *i*+1-subinterval, it is necessary to know a priori the switching moments z_{k1} and z_{k2} corresponding to the switching moments t_{k1} and t_{k2} in absolute time.

The power switch turns on at the beginning of *k*-clock interval and turns off at the moment of comparing u_{rg} deployment voltage and u_{con} control signal (Figure 1, b). This switching moment (z_{k1}) can be described using the switching manifold equation

$$\xi_1(\mathbf{X},z) = \alpha\left(u_{ref} - \mathbf{c}_{s1}\mathbf{Y}(z)\right) + u_{prb}(t) - U_{rgm}z = 0, \tag{7}$$

where $\xi_1(\mathbf{X},z)$ is the switching function (up to the switching moments z_{k1} $\xi_1(\mathbf{X},z)>0$, after the the switching moments z_{k1} $\xi_1(\mathbf{X},z)<0$), $\mathbf{c}_{s1}=(1\ 0)$ is the row-vector – select line of a given component from output vector $\mathbf{Y}$ (in this case u_{out}), U_{rgm} is the amplitude of the deployment voltage u_{rg},

$$u_{prb}(t) = u_{prbm} \sin(\omega_{prb} t) .$$

Any numerical method for solving nonlinear transcendental equations (dichotomy method, Newton's method) can be used to solve equation (7).

The switching moment of z_{k2} power diode is associated with getting by the inductor current zero, which is described by the following equation of the switching manifold

$$\xi_2(\mathbf{X}, z) = \mathbf{c}_{s2}\mathbf{Y}(z) = 0,$$

where $\xi_2(\mathbf{X},z)$ is the switching function, $\mathbf{c}_{s2}$=(0 1) is the row-vector – i_L selection line from output vector **Y**. This equation is also solved using one of the previously mentioned numerical methods.

When constructing a given frequency response, the amplitude of one of the measuring actions (u_{prbm}, j_{outvm}, u_{invm}) has a given non-zero value, and the amplitudes of the remaining pulses are zero and the calculation of time dependencies is carried out according to expression (6) with the calculation of switching moments at the beginning of each clock interval. After obtaining the time dependence of the signal from a given output, Fourier analysis of the input measuring action and the output signal is performed in order to calculate the amplitudes and phases of the harmonic with ω_{prb} frequency, after which the modulus and phase of the ratio of the output physical quantity to the input monitoring pulse are calculated. The model in question was implemented in C++, which allowed for high calculation speed.

4 Modelling results

This part presents the results of calculating the frequency characteristics obtained using the developed mathematical model of a direct inverting converter with generators of measuring actions. Converter parameters are the following: U_{in}=100 V, R_L=0.2 Ohm, L=0.0075 H, R_c=0.01 Ohm, C=50 uF, R_{vdon}=0.01 Ohm, R_{vdoff}=10^6 Ohm, R_{vton}=0.01 Ohm, R_{vtoff}=10^6 Ohm, α=1, β=-0.005, U_{rgm}=10 V, u_{ref}=7.67 V, T=0.0001 s. Measuring action amplitudes are u_{prbm}=0.015 V, j_{outvm}=0.015 A, u_{invm}=2 V.

The calculation results are shown in Figure 3.

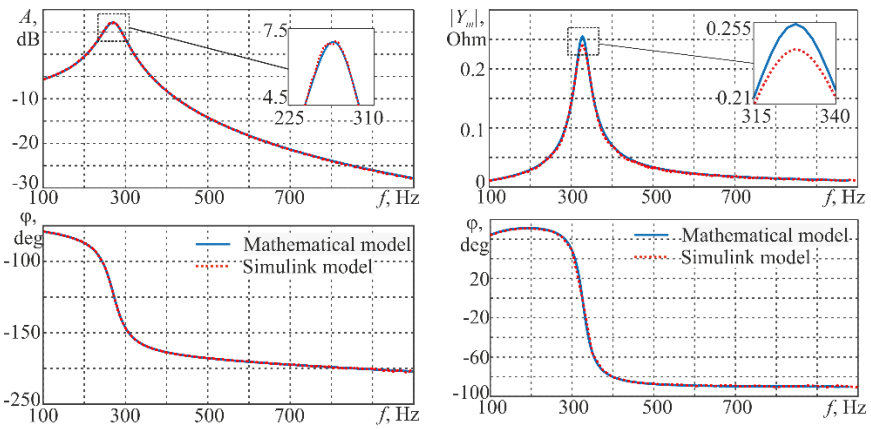

(a) (b)

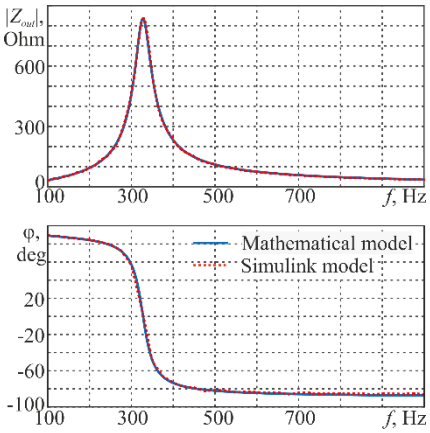

Fig. 3. Explanation of the equivalent circuit: (a) – equivalent circuit structure, (b) – time diagrams of the system signals.

At the same time, they are combined with the calculation results obtained using MatLab Simulink 2009 converter model and Simulink measuring module previously developed by the author [15]. MatLab Simulink model also belongs to the class of nonlinear dynamic models, which makes this comparison correct. When using both models, the time integration step was 10^{-8} seconds, and the duration of the time series was 3000 PWM clock intervals.

As can be seen from the figure, the results obtained using the developed model and the model in the certified MatLab Simulink 2009 software coincide with sufficient accuracy, which indicates the correctness of the developed model. At the same time, the calculation speed has increased 5 times compared to the speed provided by MatLab Simulink 2009. This is due to both the specific features of the mathematical model, which is analytical on the basis of the invariance of the power section structure, and the implementation of this model in C++ and, accordingly, the narrow specialization of this program.

Obviously, the advantages of mathematical modeling mentioned make it more preferable if, at the stage of studying such systems, repeated construction of frequency responses with different system parameters is required.

5 Conclusion

The study of SSS frequency characteristics is an urgent task at the design stage, which allows to select scientifically both the parameters of SSS controller and SSS for operation as a part of an aggregated power supply system. If we evaluate the set of computational problems that are solved during their development, we can conclude that in some cases the duration of calculations can be significant, which requires optimization of approaches to constructing frequency characteristics using numerical experiment. The most resource-intensive task in this case is the task of calculating time series of given physical quantities. To accelerate this process, it is advisable to use a nonlinear dynamic mathematical model of SSS with generators of measuring actions. The proposed model made it possible to speed up the calculation of frequency characteristics significantly and at the same time obtain results that coincide with high accuracy with the results obtained in verified software. Similar approaches to solving these problems have not been considered in the literature before. It is also worth noting once again that the frequency characteristics obtained using the proposed model will be more accurate than the characteristics obtained using analytical expressions, since the

developed model is of nonlinear dynamic type. This approach can be extended to other types of pulse converters after correcting the mathematical model.

References

1. R.P. Severns, G. Bloom, *Modern DC-to-DC Switchmode Power Converter Circuits* (New York, Van Nostrand Reinhold Company, 1985).
2. M. Rashid, *Power Electronics Handbook* (Butterworth-Heinemann, 2010).
3. V.F. Dmitrikov, D.V. Shushpanov, A.Y. Petrochenko, M.A. Alekseev, Russ. Electrical Eng. **91**, 108 (2020).
4. G.A. Belov, *Semiconductor Converter Control Systems* (Cheboksary, Chuvash State University Publ., 2023).
5. K.J. Astrom, B. Wittenmark, *Computer Controlled Systems* (New Jersey, Prentice-Hall, 2011).
6. R.D. Middlebrook, *Input Filter Considerations in Design and Application of Switching Regulators,* in Proceedings IEEE Industry Applications Society Annual Meeting, October 1976, Chicago, IL (1976).
7. Zh.T. Zhusubaliyev, E.A. Soukhoterin, E. Mosekilde, J. IEEE Trans. on Circuits and Systems I: Fundamental Theory and Appl. **50**, 1047 (2003).
8. S. Li, B. Fahimi, *On the Period-doubling Bifurcation in PWM controlled Buck Converter*, in Proceedings in Proceedings IEEE Transportation Electrification Conference and Expo, ITEC, 13-15 June 2018, Long Beach, CA, USA (2018).
9. A.I. Andriyanov, *Development of the theory of control of nonlinear dynamic processes of pulsed power supply systems* (Bryansk, 2022).
10. S.G. Mikhalchenko, V.I. Apasov, *Applying a mathematical model for determining power section ratings of a buck-boost converter*, in Proceedings International Conference of Young Specialists on Micro/Nanotechnologies and Electron Devices, EDM, 30 June - 4 July 2016, (Erlagol, Russia, 2016).